

Design of TiO₂-Based Hybrid Systems with Multifunctional Properties

Simona Ortelli , Maurizio Vespignani, Ilaria Zanoni, Magda Blosi, Claudia Vineis, Andreana Piancastelli, Giovanni Baldi, Valentina Dami, Stefania Albonetti and Anna Luisa Costa

Supplementary Materials

Table S1. Sample codes and TiO₂:LP weight ratios of nanosols obtained via the sol-gel synthesis process and relative powders obtained via the SFD process.

Sample Code		TiO ₂ :LP Weight Ratio
Nanosol	Powder	
TiO ₂ @LP_1:0.1_S	TiO ₂ @LP_1:0.1_S_SFD	10.0
TiO ₂ @LP_1:0.5_S	TiO ₂ @LP_1:0.5_S_SFD	2.0
TiO ₂ @LP_1:1_S	TiO ₂ @LP_1:1_S_SFD	1.0
TiO ₂ @LP_1:2_S	TiO ₂ @LP_1:2_S_SFD	0.5
TiO ₂ @LP_1:6_S	TiO ₂ @LP_1:6_S_SFD	0.17
TiO ₂ @LP_1:8_S	TiO ₂ @LP_1:8_S_SFD	0.13
TiO ₂ @TX_S	TiO ₂ @TX_S_SFD	16.7 *

* TiO₂:Triton X weight ratio.

Table S2. Sample codes and TiO₂:LP weight ratios of nanosols obtained via the heterocoagulation process and relative powders obtained via the SFD process.

Sample Code		TiO ₂ :LP Weight Ratio
Nanosol Sample	Powder Sample	
TiO ₂ /LP_1:1_E	TiO ₂ /LP_1:1_E_SFD	1.0
TiO ₂ /LP_1:6_E	TiO ₂ /LP_1:6_E_SFD	0.17
TiO ₂ /LP_1:8_E	TiO ₂ /LP_1:8_E_SFD	0.13

The TiO₂ used to produce the heterocoagulated samples is TiO₂@TX_S of Table S1 (containing around 6 wt.% of Triton X).

Table S3. Adsorption properties derived by UV-Vis analysis.

Powder Sample Code	Absorption Range (nm)	Band Gap Energy (eV)
TiO ₂ @TX_SFD	350–450	3.14
TiO ₂ P25 *	350–420	3.19
TiO ₂ @LP_1:0.1_S_SFD	350–420	3.17
TiO ₂ @LP_1:0.5_S_SFD	350–420	3.18
TiO ₂ @LP_1:1_S_SFD	350–420	3.18
TiO ₂ @LP_1:2_S_SFD	300–380	3.33
TiO ₂ @LP_1:6_S_SFD	300–360	3.41
TiO ₂ @LP_1:8_S_SFD	300–360	3.41

* TiO₂ P25 (commercial powder sample from Degussa-Evonik).

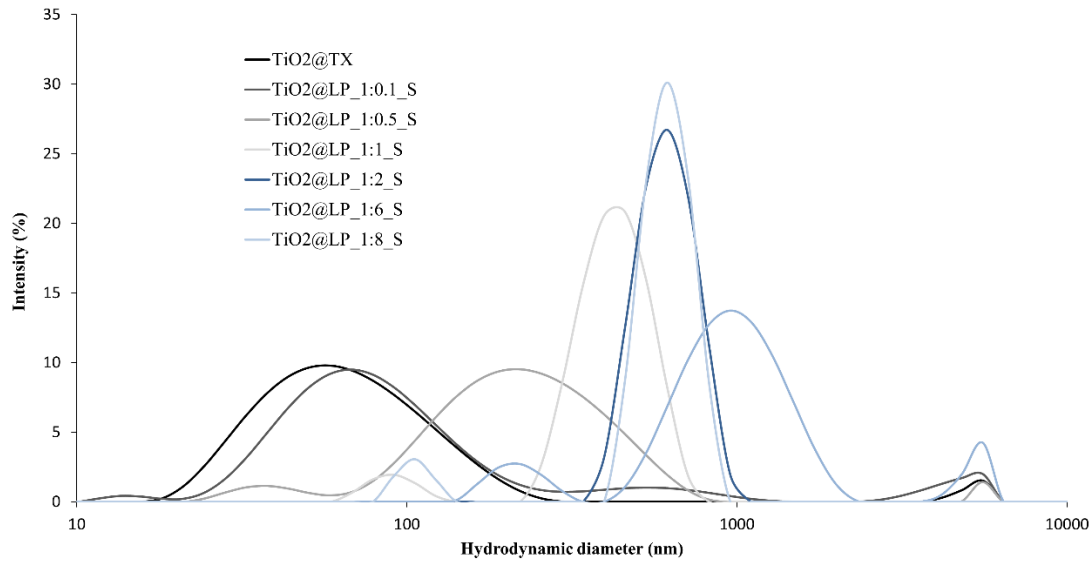


Figure S1. Particle size distribution of TiO₂@LP samples obtained via the sol–gel synthesis method.

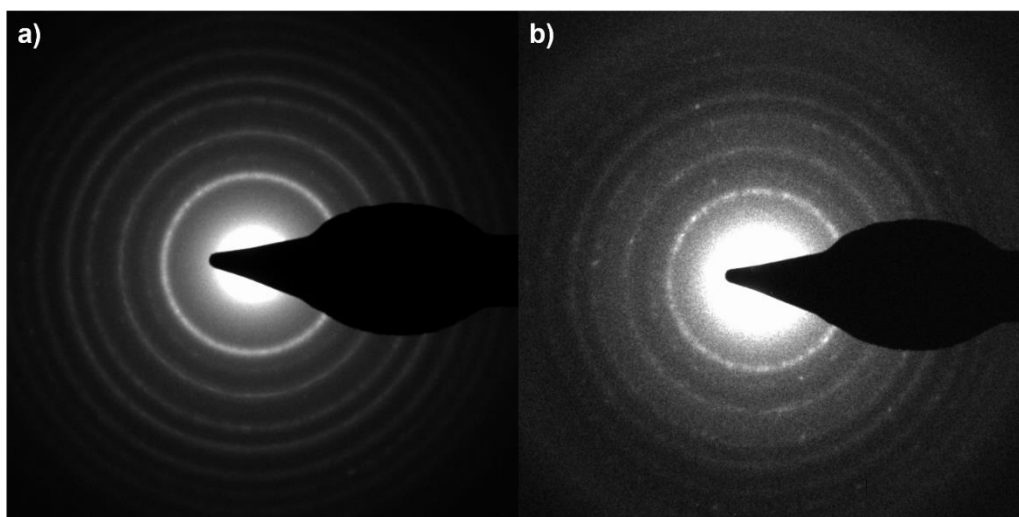


Figure S2. SAED patterns of the (a) $\text{TiO}_2@\text{LP}_\text{S}$ 1:0.1 and (b) $\text{TiO}_2@\text{LP}_\text{S}$ 1:1 samples.

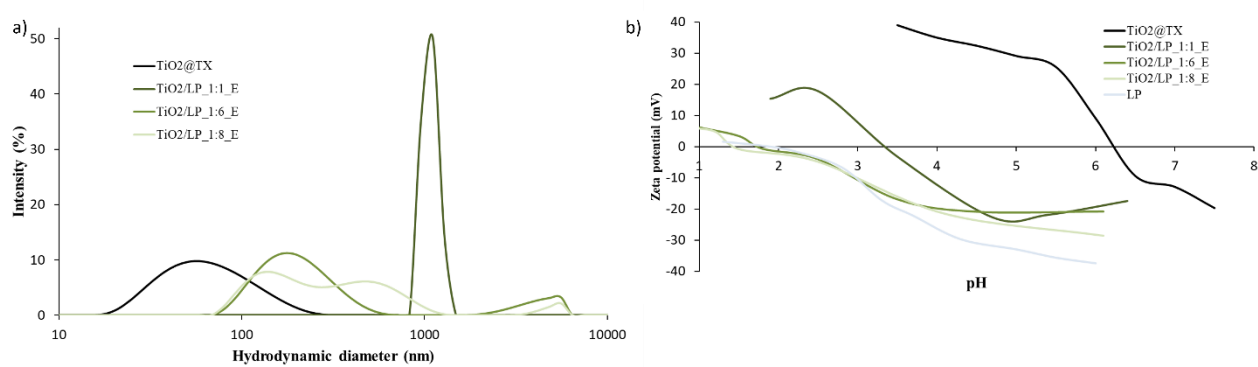


Figure S3. (a) Particle size distribution and (b) Zeta potential as a function of pH curves of $\text{TiO}_2/\text{LP}_\text{E}$ samples obtained via the heterocoagulation process.

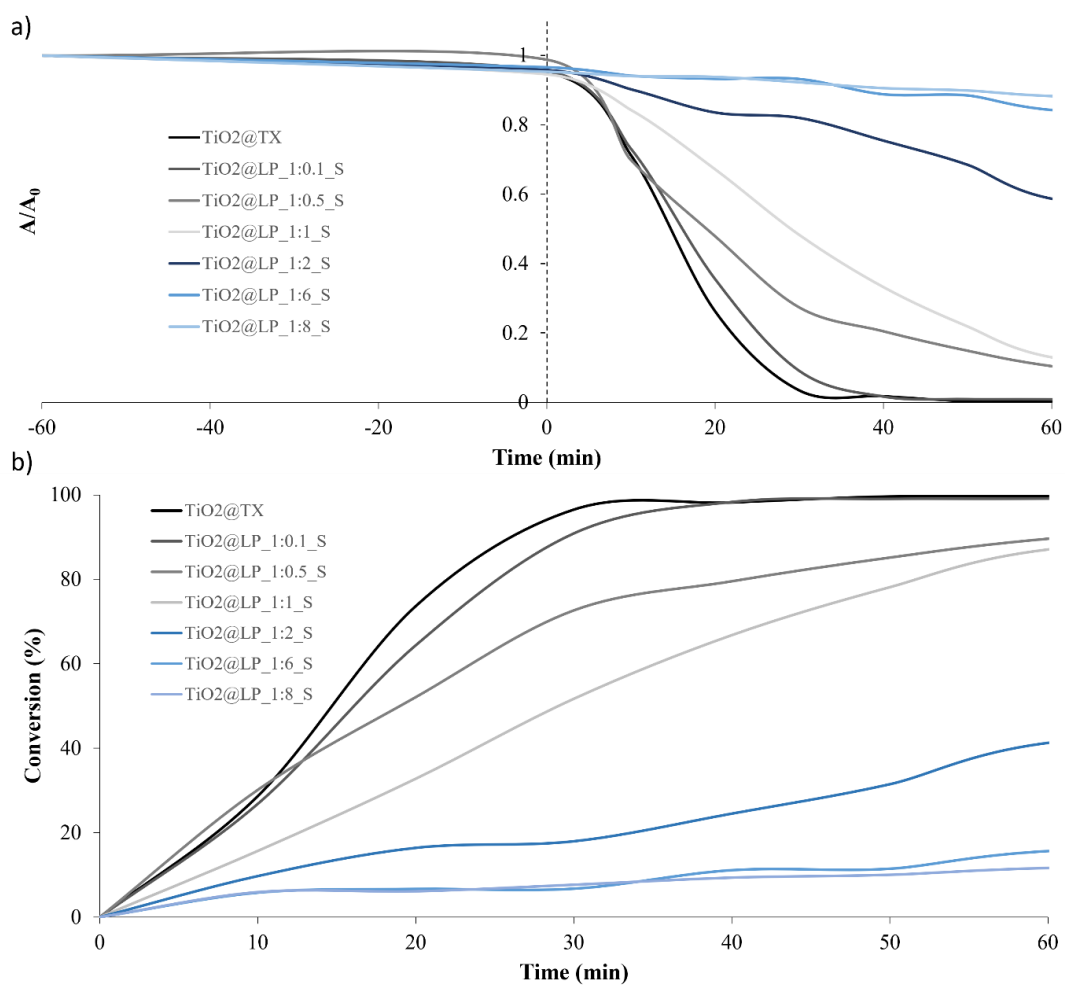


Figure S4. (a) Trends of A/A_0 and (b) conversion (%) over time for $\text{TiO}_2@\text{LP}_S$ samples obtained via the sol-gel synthesis method.

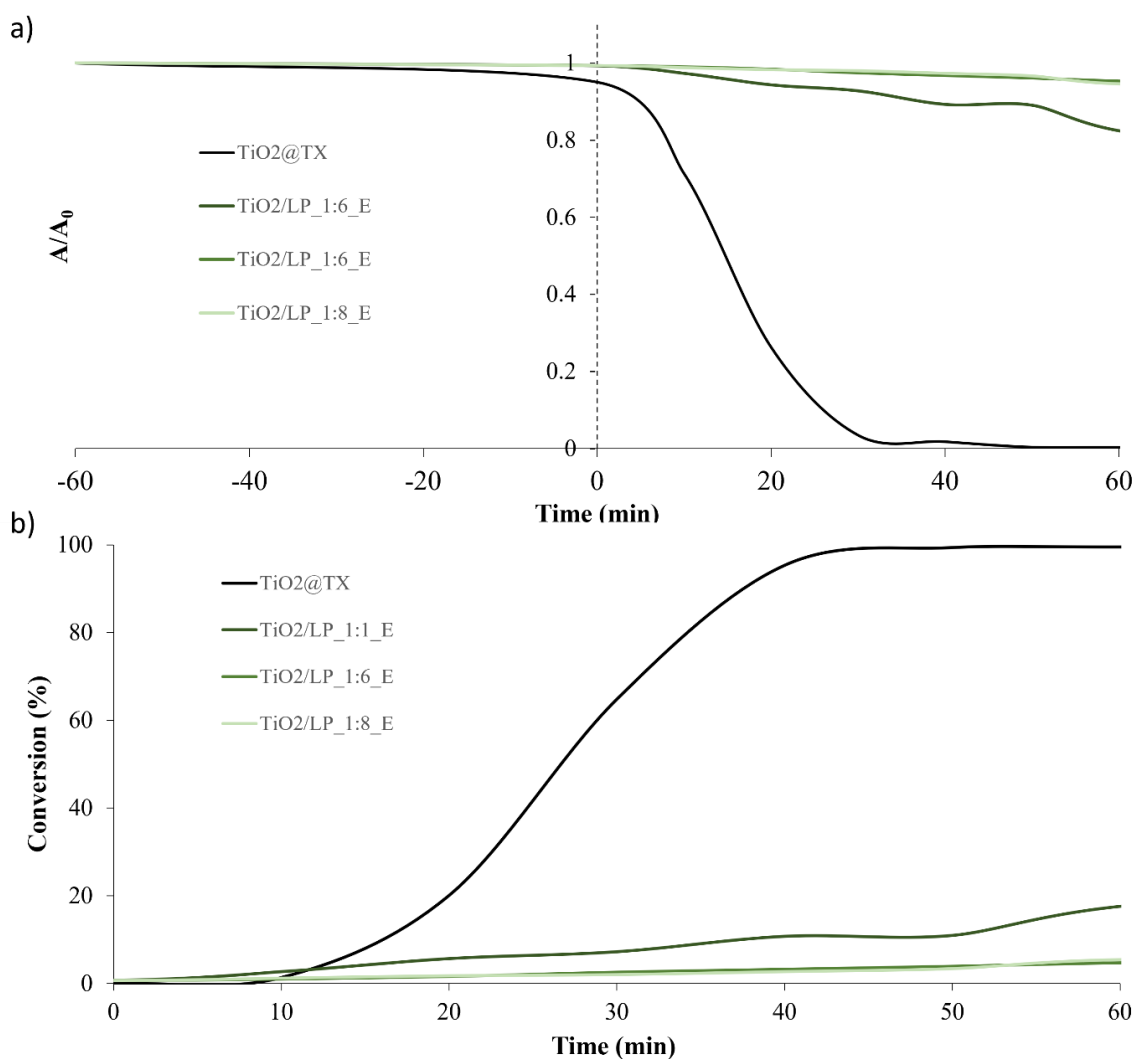


Figure S5. (a) Trends of A/A_0 and (b) conversion (%) over time for TiO₂/LP_E samples obtained via the heterocoagulation process.

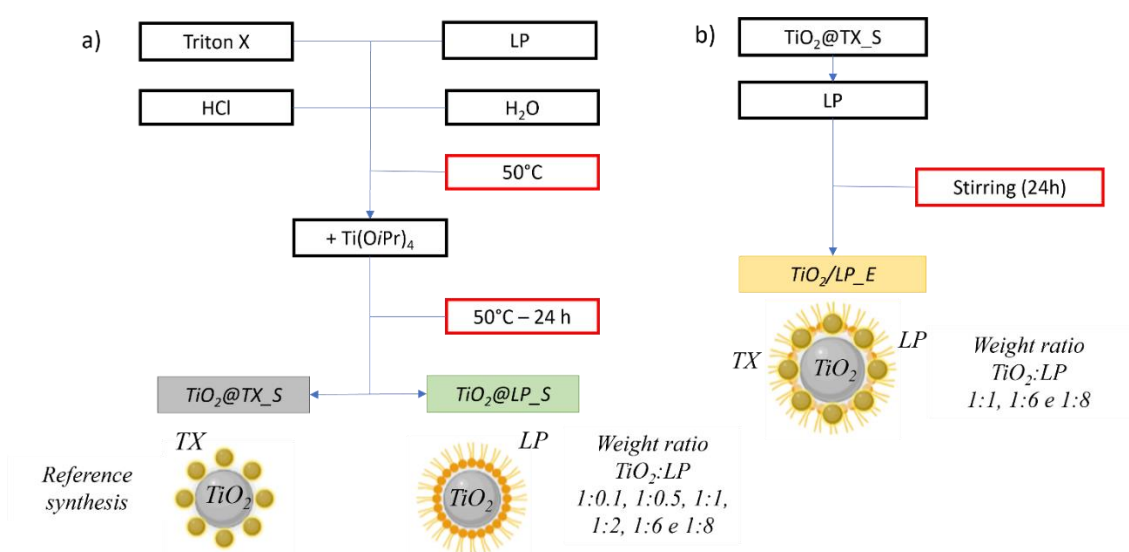


Figure S6. Scheme of (a) sol-gel processes using Triton X (TX) and mixture of lipopeptides (LP) as a surfactant and (b) the heterocoagulation process.

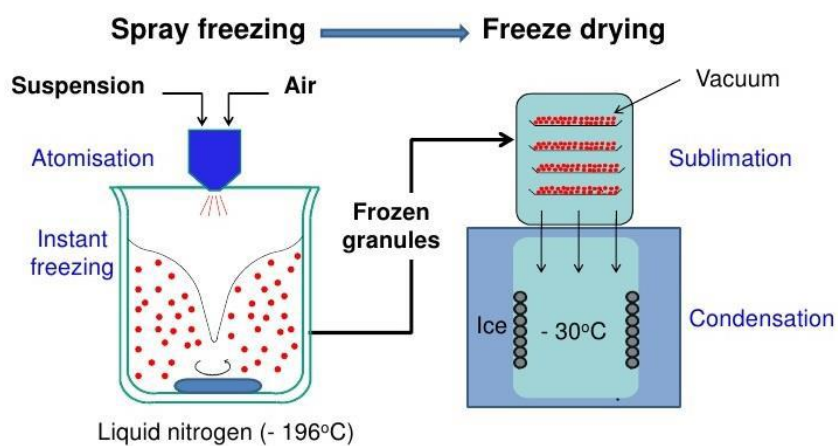


Figure S7. Schematisation of the spray-freeze-drying process.

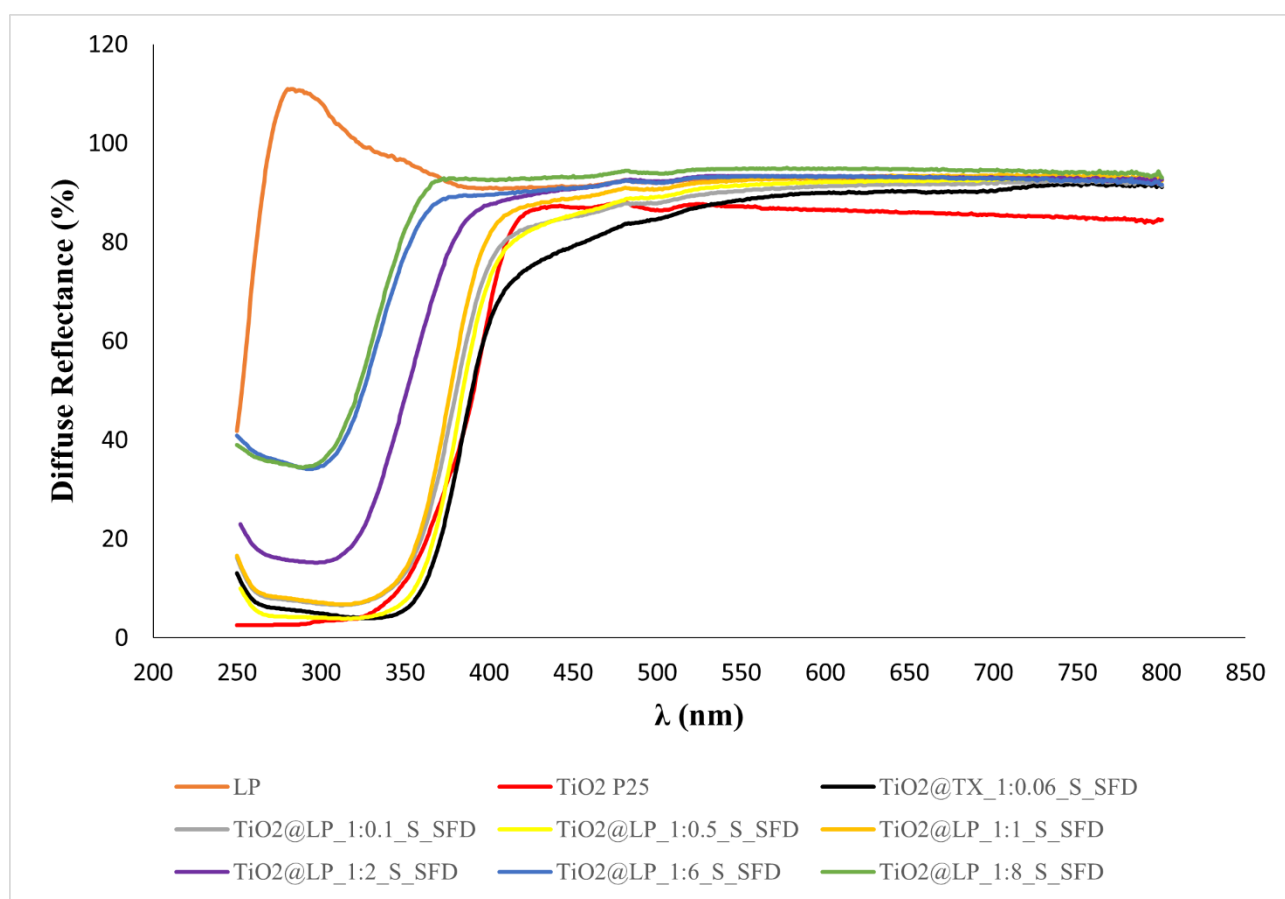


Figure S8. Diffuse reflectance over different wavelengths of $\text{TiO}_2@\text{LP}_\text{S}$ samples.